

# X-ray harmonics rejection on third-generation synchrotron sources using compound refractive lenses

Maxim Polikarpov,<sup>a,b</sup> Irina Snigireva<sup>b</sup> and Anatoly Snigirev<sup>b\*</sup>

<sup>a</sup>National Research Nuclear University 'Mephi', 31 Kashirskoe Shosse, 115409 Moscow, Russian Federation, and <sup>b</sup>European Synchrotron Radiation Facility, 6 rue Jules Horowitz, 38043 Grenoble, France. \*E-mail: snigirev@esrf.fr

Received 10 December 2013

Accepted 15 January 2014

A new method of harmonics rejection based on X-ray refractive optics has been proposed. Taking into account the fact that the focal distance of the refractive lens is energy-dependent, the use of an off-axis illumination of the lens immediately leads to spatial separation of the energy spectrum by focusing the fundamental harmonic at the focal point and suppressing the unfocused high-energy radiation with a screen absorber or slit. The experiment was performed at the ESRF ID06 beamline in the in-line geometry using an X-ray translocator with compound refractive lenses. Using this technique the presence of the third harmonic has been reduced to  $10^{-3}$ . In total, our method enabled suppression of all higher-order harmonics to five orders of magnitude using monochromator detuning. The method is well suited to third-generation synchrotron radiation sources and is very promising for the future ultimate storage rings.

© 2014 International Union of Crystallography

**Keywords:** X-ray refraction; focusing; X-ray refractive lenses; harmonic suppression.

## 1. Introduction

Currently, experiments performed on synchrotron radiation sources normally use high photon intensity/brilliance of the source with a double-crystal monochromator utilizing various orders of diffraction [e.g. Si(111), Si(220)]. As monochromators select from a given spectrum a series of harmonics whose wavelengths satisfy Bragg's law for the monochromator diffracting planes, higher-order harmonics are still present in the spectrum after monochromatization with not negligible relative intensities. As a consequence, X-ray harmonics rejection is an essential part of most experiments with synchrotron radiation where a specified and single wavelength is required (e.g. XAFS).

The two most important existing approaches for rejecting higher harmonics are crystal detuning of double-crystal monochromators and the use of grazing-incidence mirrors.

First, as the bandwidth of the fundamental reflection is appreciably larger than the bandwidth of higher-order harmonics, one crystal can be slightly moved ('detuned') out of the parallel position with respect to the other crystal. This suppresses higher-order harmonics (Bonse *et al.*, 1976). Independent of energy, the minimum harmonic contamination is about  $10^{-2}$  where the remaining fundamental harmonic fluxes are about 50% (Hou, 2005).

The second well known optical element for harmonics rejection is a grazing-incidence mirror (Hastings *et al.*, 1978; Latimer *et al.*, 1995; Lambie, 1995), which is mostly used in

conjunction with monochromator detuning. The mirror can be aligned at a certain angle such that only X-rays below a specific energy are transmitted through (after) the crystal monochromator. This method shows higher-order harmonics suppression down to  $10^{-4}$ – $10^{-5}$  and even  $10^{-6}$  in the case of multilayer monochromators (Lingham *et al.*, 1996).

There are also other techniques for specific harmonic selection, such as using asymmetric bent Laue Si crystals (Karanfil *et al.*, 2004), which is well suited to XAFS; or harmonic suppression by undulator segmentation (Tanaka & Kitamura, 2002), which is similar to the detuning technique.

All the above techniques, based on reflective optics and crystals, have a number of major disadvantages: they are difficult to install, align and obtain results; they also change the direction of the beam's propagation during numerous reflections. Moreover, in the case of mirrors, the surface quality and angular tuning needs to be almost perfect. Whereas the monochromator detuning technique is easier, it often cannot provide the desirable harmonics rejection. In this paper we would like to introduce a new in-line method of harmonic rejection based on X-ray refractive lenses (Snigirev *et al.*, 1996) or X-ray translocators (Snigirev *et al.*, 2009a). Since their development in 1996, X-ray refractive lenses have become standard elements in synchrotron beamline instrumentation enabling the focusing of high-energy radiation from the microscale to the nanoscale. This has extended the potential of a variety of research techniques including X-ray nano-interferometry (Snigirev *et al.*, 2009b), high-resolution

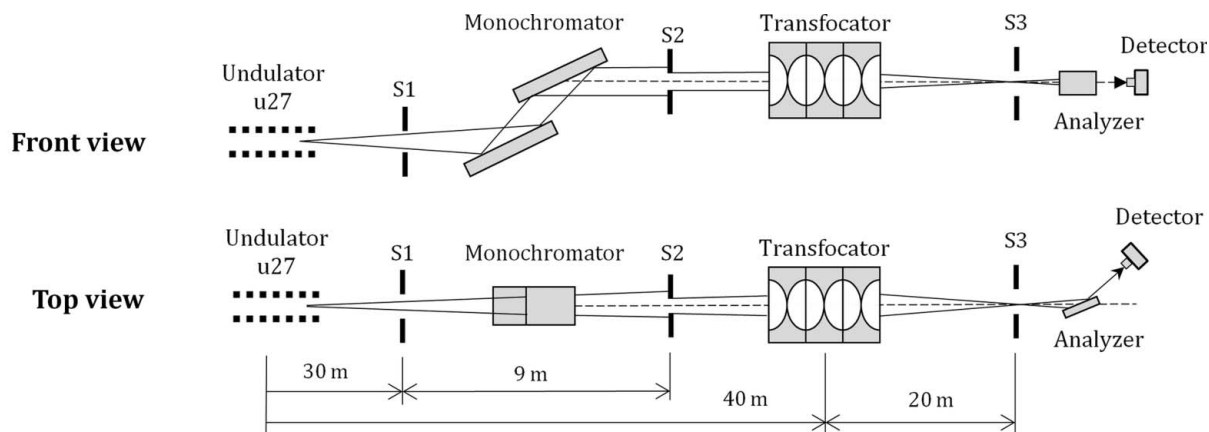


**Figure 1**  
Layout of the experiment on the X-ray harmonics rejection at the ID06 beamline, ESRF.

microscopy (Lengeler *et al.*, 1999) and standing-wave microscopy (Drakopoulos *et al.*, 2002). X-ray transfocators, where the focal distance can be continuously adjusted by insertion or retraction of one or more lens cartridges, in turn have played a major role in this development over the last few years. Transfocators are now widely used on most beamlines of third-generation synchrotrons such as ESRF (Vaughan *et al.*, 2011) or PETRA-III (Zozulya *et al.*, 2012). Based on transfocators, the new harmonic rejection technique that we propose expands the list of their applications and facilitates the experiments carried out on synchrotron sources. Since the index of refraction for X-rays in matter can be written as  $n = 1 - \delta + i\beta$ , where  $\beta$  is the absorption index and  $\delta$  is the energy-dependent refractive index decrement, this leads to the fact that the focal distance of the compound refractive lens (CRL; Lengeler *et al.*, 2005) is energy-dependent as well:  $F = R/2N\delta$ , where  $R$  is the radius of the lens and  $N$  is the number of lenses in the CRL. Therefore, the use of an off-axis illumination of the CRL, *i.e.* the offset of the beam from the principal axis of the lens, allows us to spatially split an energy spectrum by focusing the main harmonic at the focal point and suppressing the unfocused high-energy radiation with a screen absorber or slit.

## 2. Experiment

The experiment was performed at the Micro Optics Test Bench (Snigirev *et al.*, 2007) at ID06 beamline at the ESRF in Grenoble, France. This is an undulator beamline with a source size of 25  $\mu\text{m}$  (FWHM) and 900  $\mu\text{m}$  (FWHM) in the vertical and horizontal directions, respectively.

The layout of the experiment is shown in Fig. 1. The primary slits (S1) were chosen to be 0.5 mm in both directions to collimate the X-radiation. The 9 keV X-rays were selected by a cryogenically cooled Si(111) double-crystal monochromator. The essential part of the set-up is the transfocator, a

device where the focal distance can be continuously adjusted by insertion or retraction of one or more of the lens cartridges, which is installed in the path of the beam after the monochromator. Since it consists of cartridges with a variable number of beryllium parabolic refractive lenses, we used the configuration of nine lenses of radius  $R = 1$  mm set as a CRL to obtain the desirable imaging distance  $L_2 = 20$  m for the energy  $E = 9$  keV. We would like to mention that the effective aperture ( $A_{\text{eff}}$ ) of such a CRL is 1.6 mm (Snigirev *et al.*, 1996).

As discussed earlier, the spectrum after the monochromatization by Si(111) crystals consists of the fundamental harmonic, 111, and higher-order harmonics, 333, 444 *etc.* The contribution to harmonics contamination comes mainly from the third harmonic with energy  $E = 27$  keV. Clearly, by inserting the transfocator into the beam the fundamental harmonic with energy of 9 keV is focused on a principal axis whereas higher-order harmonics continue to pass almost straight ahead (Fig. 2). To make a spatial separation of these parts of the spectrum we use an off-axis illumination geometry, which was realised by means of secondary slits (S2). They were set with a vertical offset  $\Delta z$  of the incident beam from the principal axis. The opening of the secondary slits (S2vg) has to be at least less than  $A_{\text{eff}}/2$  of the lenses to provide the efficient spatial separation of undesirable harmonics. Nevertheless, to insure ourselves, the slits gap was chosen to be about 0.2 mm (S2vg = 0.2 mm). The third slits (S3) were used to suppress the unfocused higher-energy radiation. To evaluate the efficiency of the higher-order harmonics suppression we used the Si(111) analyzer crystal in the Bragg geometry, which was installed

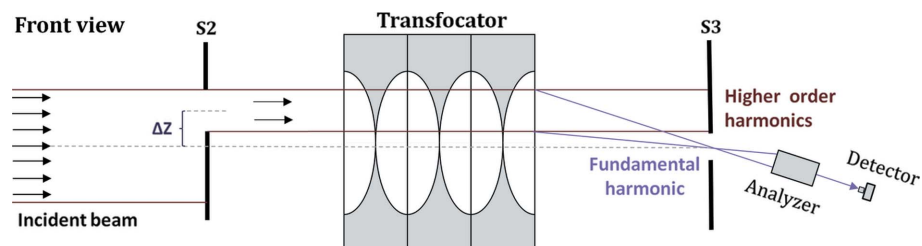


**Figure 2**  
Optical geometry of the X-ray harmonics rejection.

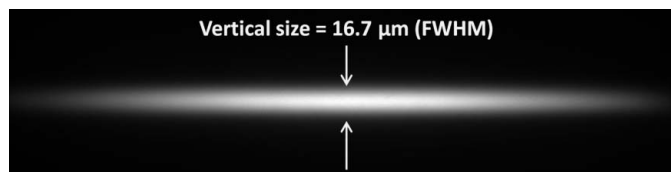


**Figure 3**  
Image of the source, focused by the translocator. The vertical size of the image is 16.7  $\mu\text{m}$  (FWHM), which corresponds to an initial source size of 25  $\mu\text{m}$ .

after the focusing point of the translocator. Rocking-curve scans were performed at the fundamental harmonic ( $E = 9$  keV) and at the third harmonic ( $E = 27$  keV), while the intensity was measured using a detector (PIN diode), installed right after the crystal. The measurements were performed with and without vertical offset  $\Delta z$  of the S2 slits.

We also tested the focusing properties of the translocator by placing a high-resolution CCD camera (0.56  $\mu\text{m}$  pixel size) at its imaging distance. The spot size in the vertical direction was 16.7  $\mu\text{m}$  (FWHM) which corresponds to an initial source size of 25  $\mu\text{m}$  (FWHM). The recorded image is shown in Fig. 3.

The rocking-curve scans of the analyzer crystal at the fundamental and at the third harmonics (corresponding to energies of 9 keV and 27 keV, respectively) for the in-line geometry without S2 slits offset are depicted in Fig. 4. Identical

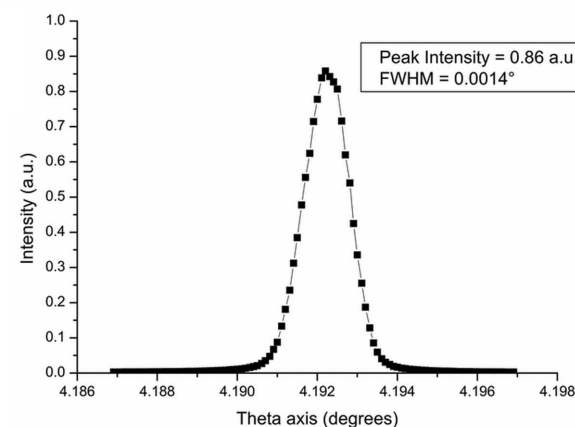
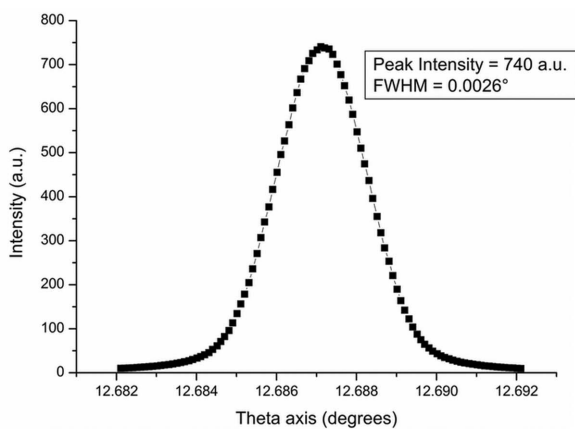


**Figure 4**  
Rocking curves of the Si(111) analyzer at the fundamental harmonic ( $E = 9$  keV), top, and at the third harmonic ( $E = 27$  keV), bottom, measured without a vertical offset ( $\Delta z = 0$ ).

tical analyzer's rocking-curve scans at the fundamental and at the third harmonics using off-axis illumination (with the S2 slits offset  $\Delta z$  of 0.3 mm) are plotted in Fig. 5. The S2 and S3 slits opening gaps in the vertical and horizontal directions were 0.2 mm. The width of the rocking curves (FWHM) at the fundamental and at the third harmonics was of the order of 0.0026° and 0.0015°, respectively, for both the in-line geometry and the off-axis translocator illumination. This shows that the off-axis illumination does not disturb the properties of the incoming beam. It should be noted that the intensity at the fundamental harmonic dropped by a factor of five using the off-axis geometry. To estimate the level of high-order harmonics attenuation we used the ratio of the intensities  $I_2/I_1$ , where  $I_2$  is the peak intensity of the analyzer's rocking curve for the appropriate energy with offset  $\Delta z = 0.3$  mm, and  $I_1$  is the peak intensity of the analyzer's rocking curve for the appropriate energy without offset, *i.e.*  $\Delta z = 0$ . As can be seen from a comparison of Figs. 4 and 5, we achieve a suppression of the third harmonic of the order of  $10^{-3}$ .

Similar measurements were performed for different S3vg openings and the results are presented in Table 1. As indicated in the table, the harmonics rejection level becomes better by decreasing the S3 slits gap size while the main harmonic intensity decreases insignificantly. This happens because the beam is highly focused (the spot size is  $<20$   $\mu\text{m}$ ) by the CRL

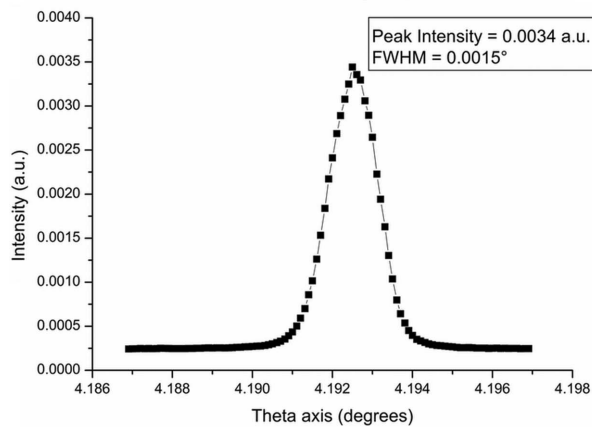
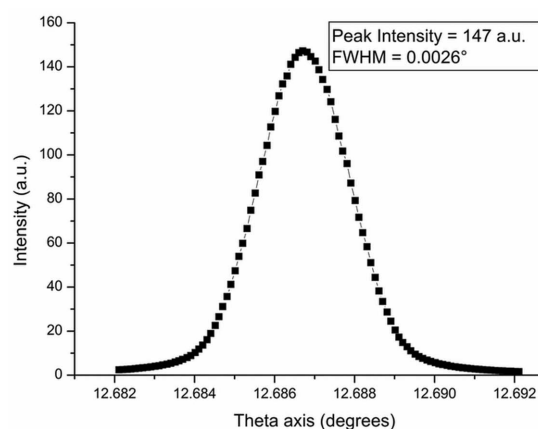


**Figure 5**  
Rocking curves of the Si(111) analyzer at the fundamental harmonic ( $E = 9$  keV), top, and at the third harmonic ( $E = 27$  keV), bottom, measured with a vertical offset  $\Delta z = 0.3$  mm.

**Table 1**

Harmonics rejection by the CRL.

$I_2$  is the peak intensity of the analyzer's rocking curve for the appropriate energy with offset ( $\Delta z = 0.3$  mm).  $I_1$  is the peak intensity of the analyzer's rocking curve for the appropriate energy without offset ( $\Delta z = 0$ ).

Spectral component (keV)	$I_2/I_1$	S2 slits vertical gap (mm)	S3 slits vertical gap (mm)
9	0.2	0.2	0.2
	0.18	0.2	0.1
	0.14	0.2	0.05
27	$4 \times 10^{-3}$	0.2	0.2
	$2.5 \times 10^{-3}$	0.2	0.1
	$1 \times 10^{-3}$	0.2	0.05

and closing the S3 slits leads to suppression of useless radiation (including higher-order harmonics), scattered by air. Therefore, higher-order harmonics suppression is highest in cases where the S3 slits gap size is set to the order of the image size of the focused beam.

Thus, the level of higher-order harmonics suppression using the proposed technique is of the order of  $10^{-3}$  with a total throughput of  $\sim 20\%$  at the fundamental. In addition, we would like to note that monochromator detuning by  $0.0005^\circ$  suppresses the third harmonic to  $10^{-2}$  by reducing the fundamental by a factor of 1.4. As a result, our method coupled with monochromator detuning enabled suppression of all higher-order harmonics to five orders of magnitude with a total throughput of  $\sim 14\%$  at the fundamental.

### 3. Discussion and conclusion

A novel technique of suppressing higher-order harmonics based on refractive optics was proposed. As shown, CRLs used in off-axis illumination can reject higher-order harmonics down to  $10^{-5}$ . In parallel with the harmonic suppression the refractive lenses can be applied for many other types of synchrotron experiments including microfocusing and imaging. In contrast, monochromator detuning attenuates unwanted harmonics only down to  $10^{-2}$  while grazing mirrors suppress them down to  $10^{-4}$ – $10^{-5}$ . Mirrors retain 80–90% of the flux at the fundamental harmonic and show the same degree of harmonics rejection as the technique proposed here, which makes mirrors effective in the energy region up to 20 keV.

However, we would like to stress that the CRL-based method of eliminating undesirable energies in terms of its performance is preferable at higher energies up to 100 keV, where the mirror's efficiency recedes due to decreasing grazing angle and reduced acceptance. In addition, mirrors, as well as all reflective optical elements, change the direction of the beam propagation, making them difficult to align. Due to numerous reflections from the surfaces of the mirrors, beam properties such as coherence become significantly deteriorated. The refractive lenses are used in the inline geometry that allows the coherency of the beam to be much better preserved. Besides, CRLs are user-friendly in terms of installation, alignment and performing the experiments.

In our experiment, because of the design of ID06 at ESRF, the transfocator was placed at 38 m from the source and, as a result, intensity loss occurred due to beam divergence. However, the described harmonics rejection technique could be realised in a more efficient way at beamlines if the transfocator is moved closer to the source (Vaughan *et al.*, 2011). In the near future new fourth-generation synchrotrons (MAX IV, NSLS-II) and upgraded third-generation synchrotrons (ESRF, SPring-8 and APS) will come with unprecedented beam brilliance, coherence and drastically reduced horizontal emittance. This brings the possibility of increasing the acceptance of CRLs by using the full beam and reducing intensity losses.

Additionally, our technique can be improved by using an annular illumination instead of off-axis illumination. Inserting a central beam-stop of size equal to twice the  $\Delta z$  offset would increase the flux of the fundamental harmonic by a factor of two, retaining the same level of harmonic suppression.

The authors are very grateful to ID06 beamline staff for help in performing experiments, especially to C. Detlefs and P. Wattecamps. The work is supported by the Ministry of Education and Science of the Russian Federation (contract Nos. 14.Y26.31.0002 and 02.G25.31.0086).

### References

- Bonse, U., Materlik, G. & Schröder, W. (1976). *J. Appl. Cryst.* **9**, 223–230.
- Drakopoulos, M., Zegenhagen, J., Snigirev, A., Snigireva, I., Hauser, M., Eberl, K., Aristov, V., Shabelnikov, L. & Yunkin, V. (2002). *Appl. Phys. Lett.* **81**, 2279–2281.
- Hastings, J., Kincaid, B. & Eisenberger, P. (1978). *Nucl. Instrum. Methods*, **152**, 167–171.
- Hou, Z. (2005). *Rev. Sci. Instrum.* **76**, 013305.
- Karanfil, C., Chapman, D., Segre, C. U. & Bunker, G. (2004). *J. Synchrotron Rad.* **11**, 393–398.
- Lamble, G. M. (1995). *Rev. Sci. Instrum.* **66**, 1422.
- Latimer, M. J., Rompel, A., Underwood, J. H., Yachandra, V. K. & Klein, M. P. (1995). *Rev. Sci. Instrum.* **66**, 1843.
- Lengeler, B., Schroer, C. G., Kuhlmann, M., Benner, B., Günzler, T. F., Kurapova, O., Zontone, F., Snigirev, A. & Snigireva, I. (2005). *J. Phys. D*, **38**, A218–A222.
- Lengeler, B., Schroer, C. G., Richwin, M., Tümmeler, J., Drakopoulos, M., Snigirev, A. & Snigireva, I. (1999). *Appl. Phys. Lett.* **74**, 3924–3926.
- Lingham, M., Ziegler, E., Lueken, E., Loeffen, P., Mullender, S. & Goulon, J. (1996). *Proc. SPIE*, **2805**, 158–168.
- Snigirev, A., Hustache, R., Duboc, P., Massonnat, J. Y., Claustre, L., Van Vaerenbergh, P., Snigireva, I., Grigoriev, M. & Yunkin, V. (2007). *Adv. X-ray/EUV Opt. Compon. II*, **6705**, 70511.
- Snigirev, A., Kohn, V., Snigireva, I. & Lengeler, B. (1996). *Nature (London)*, **384**, 49–51.
- Snigirev, A., Snigireva, I., Kohn, V., Yunkin, V., Kuznetsov, S., Grigoriev, M. B., Roth, T., Vaughan, G. & Detlefs, C. (2009b). *Phys. Rev. Lett.* **103**, 064801.
- Snigirev, A., Snigireva, I., Vaughan, G., Wright, J., Rossat, M., Bytchkov, A. & Curfs, C. (2009a). *J. Phys. Conf. Ser.* **186**, 012073.
- Tanaka, T. & Kitamura, H. (2002). *J. Synchrotron Rad.* **9**, 266–269.
- Vaughan, G. B. M., Wright, J. P., Bytchkov, A., Rossat, M., Gleyzolle, H., Snigireva, I. & Snigirev, A. (2011). *J. Synchrotron Rad.* **18**, 125–133.
- Zozulya, A. V., Bondarenko, S., Schavkan, A., Westermeier, F., Grübel, G. & Sprung, M. (2012). *Opt. Express*, **20**, 18967–18976.